ELSEVIER

Journal of Nuclear Materials 258–263 (1998) 713–718

journal of nuclear materials

Molecular dynamics evaluation of self-sputtering of beryllium

Shuzo Ueda [a,*], Toshiro Ohsaka [b], Satoru Kuwajima [c]

[a] *Department of Fusion Technology, Naka Fusion Research Establishment, Japan Atomic Energy Research Institute, Naka-machi, Naka-gun, Ibaraki 311-01, Japan*

[b] *Applied Engineering Department, Science and Engineering Division, CRC Research Institute, Inc., 2-7-5 Minamisuna, Koto-ku, Tokyo 136, Japan*

[c] *NanoSimulation Associates, 825-1 Amado-cho, Villa D.E. 201, Hanamigawa-ku, Chiba-shi, Chiba 262, Japan*

Abstract

The self-sputtering of Be was simulated by a molecular dynamics (MD) approach with the use of a newly developed 2-body Be potential. Incident angle dependence of the sputtering yield was evaluated for the incident particle energies of 50, 100, and 300 eV with respect to the (0 0 1) and (0 1 0) surfaces of the hcp crystal. The calculated sputtering yields are in good agreement with both experimental estimates and the TRIM.SP evaluations. Small but distinct dependence on the surface type is observed. The calculated reflection coefficient become at grazing angles significantly larger than the TRIM.SP evaluation. © 1998 Elsevier Science B.V. All rights reserved.

1. Introduction

Atomic scale computer simulations such as molecular dynamics (MD) are potentially useful tools for the improved understanding and, eventually, the evaluation of fusion reactor materials, whose working environments are often difficult to probe by experimental techniques. Current atomistic MD studies targeting fusion reactor materials include the simulation of displacement cascade [1] and diffusion phenomena [2]. The subject of the present paper is sputtering; we report the MD simulation of the self-sputtering of beryllium, a candidate plasma facing material.

While the MD simulation of sputtering is an established field of research [3], its application to plasma facing materials has been rather limited. To our knowledge, MD study of Be sputtering has not been reported previously. Since the main problem in starting an MD application to a new material is the interatomic potential, one of the objectives of the present work is focused on the choice of the potential. We also outline the MD methodology and present the simulation results. Emphasis is placed on examining general aspects of the MD evaluation of sputtering rather than performing an extensive evaluation for Be.

2. Interatomic potential function

Interatomic potentials are of vital importance in atomistic simulations of materials. For Be a number of potentials have been proposed in the literature, ranging from simple 2-body potentials [4] to elaborate many-body potentials [5,6]. Those potentials, however, were developed for the study of usual low-energy phenomena and are not particularly suited for sputtering which involves orders of magnitude of higher energy than the thermal energy. For this reason we have developed a new potential for Be.

Our Be potential is a 2-body potential composed of a Moliere term [7] and an attractive function

$$u(r) = (16e_0^2/r)f(r/a) - c/(r^8 + r_0^8), \quad (1)$$

where r denotes the interatomic distance, a, c, and r_0 are fitting parameters, e_0 is the elementary charge, and f is defined by

$$f(x) = 0.35 \times 10^{-0.3x} + 0.55 \times 10^{-1.2x} + 0.1 \times e^{-6x}. \quad (2)$$

* Corresponding author. Tel.: +81-29 270 7362; fax: +81-29 270 7468; e-mail: ueda@naka.jaeri.go.jp.

0022-3115/98/$19.00 © 1998 Elsevier Science B.V. All rights reserved.
PII: S0022-3115(98)00251-7

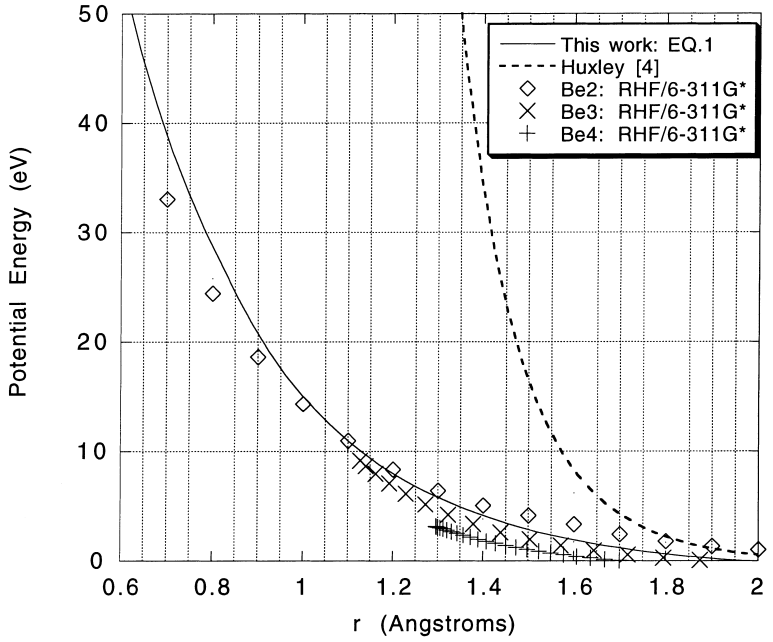

Fig. 1. Be–Be interaction potentials in small interatomic separation region.

The fitting parameters have been determined as $a = 0.1817$ Å, $c = 2835$ Å ^{8}eV, and $r_0 = 2.490$ Å.

An essential feature of Eq. (1) is its behavior at small interatomic separations (i.e., high energy region), where it is fitted to potentials obtained by ab initio quantum chemical calculations. RHF/6-311G* level of theory was applied to Be_2, Be_3, and Be_4 systems in the ab initio calculation by using a software package SPARTAN [8]. Calculated Be_n systems ($n = 3,4$) are composed of one moving atom and fixed ($n-1$) atoms which are equidis-

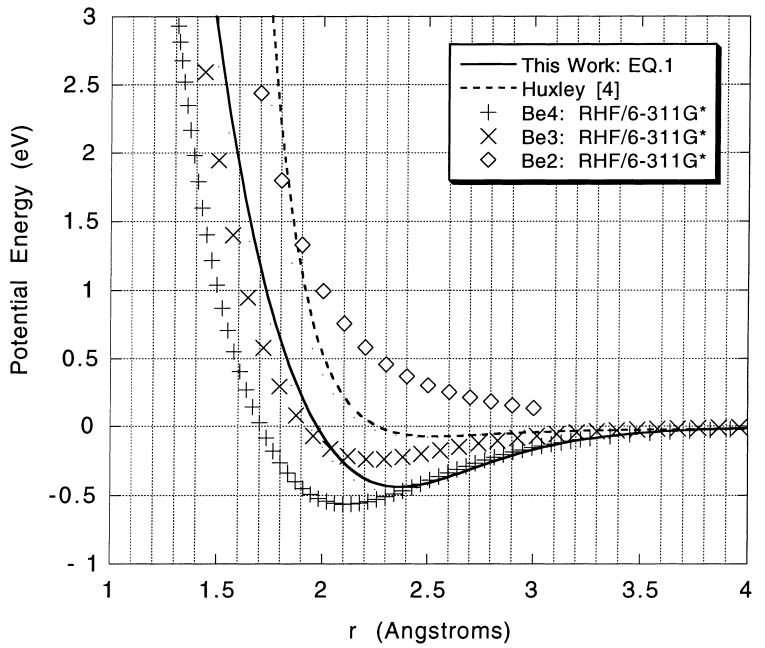

Fig. 2. Be–Be interaction potentials in medium interatomic separation region.

tant from the moving atom and 2.2446 Å apart from one another. Fig. 1 shows the potentials of Eq. (1) and the RHF/6-311G* calculations in small interatomic separation region. The Be_n potentials ($n = 3,4$) in Fig. 1 are effective 2-body potentials that are defined as $u_n(r) = [U_n(r) - U_n(\infty)]/(n-1)$, where $U_n(r)$ is the total potential energy of Be_n at distance r between the moving atom and the fixed atoms. A potential curve found in the literature [4] is also drawn in Fig. 1; this curve is an example of how much deviation can occur between a low-energy-adapted potential and (reasonably) correct potentials.

The fitting parameters of $u(r)$, Eq. (1), were determined as follows. First, the Moliere parameter a was obtained by the least square fit of the Moliere function, not the whole $u(r)$, to the quantum chemical Be_2 potentials of $r = 0.4$–3.0 Å range. Second, the r_0 and c parameters were determined so that the function $u(r)$, including the already fixed Moliere part, reproduced the experimental lattice constants and energy of the hcp crystal of Be. We actually tried 6, 8, and 10 for the exponent of r in the attractive part of $u(r)$. The exponent 8 was chosen on the ground that its potential curve was closer to the quantum chemical Be_4 curve than the other exponents. Fig. 2 shows the potential curves in medium interatomic separations. The lattice constants and energy obtained from Eq. (1) are $a = b = 2.24$ Å, $c = 3.68$ Å, and $E = 3.4$ eV as compared to the experimental values of $a = b = 2.29$, $c = 3.58$, and $E = 3.3$.

It should be remarked that the quantum chemical potentials in Fig. 2 vary drastically with the number of Be atoms. This is essentially a manifestation of many-body effects without which the potential curves should be the same. In estimating the magnitude of many-body effects from Fig. 2 we should neglect the purely repulsive RHF/ 6-311G* Be_2 curve and replace it by the curve of Huxley et al., because the latter represents, in the range of $2.30 \leqslant r \leqslant 5.29$ Å, much higher level of quantum chemical Be_2 calculations than the RHF/6-311G* method [4]. (Note that Huxley's potential becomes a totally groundless extrapolation in high energy region.) The deviations between the curves of Huxley et al., Be_3 and Be_4 are still large. Therefore, 2-body potentials for Be involve an intrinsic limitation in mimicking real Be systems. Since our potential is fitted to the crystal results and fairy close to the quantum chemical Be_4 curve, its limitation should become serious mainly in small clusters.

3. MD simulation

3.1. General methodology

MD simulation of sputtering starts with the injection of an incident particle to a target crystal [3]. We have used periodic boundary conditions, and the target crystal is an infinite plate rather than a finite microcrystal. A schematic drawing of the simulation arrangements is shown in Fig. 3. Time development of the collision process is followed by solving the classical mechanical equations of motion. We have adopted an NPE dynamics [9] in order to allow the volume relaxation of the crystal, though this choice is not common in sputtering simulations. Leap frog algorithm is used to integrate the equations of motion. The time increment is varied a few times as the maximum velocity of the atoms in the system decreases.

Our MD program was written based on a general-purpose commercial code named GEMS/MD [10]. Since 2-dimensional periodic boundary conditions are not available in GEMS/MD, we had to use 3-dimensional ones. Applying 3-dimensional periodicity in sputtering simulations can cause the collision of the sputtered atoms with the periodic images of the target crystal. This artificial effect was avoided by immobilizing outgoing atoms at some distance from the crystal surface.

3.2. Simulation conditions

The incident particle energies studied are 50, 100, and 300 eV. Angle dependence is computed for the 50 and 100 eV collisions, the incident angles being 0°, 30°, 45°, 60°, and 75°. For the 300 eV collision only the normal incidence was simulated. The crystal structure of the target Be plate was the hcp structure. Two types of the crystal surface were studied: the (0 0 1) and (0 1 0) faces. The sizes of the target crystals used are listed in Table 1.

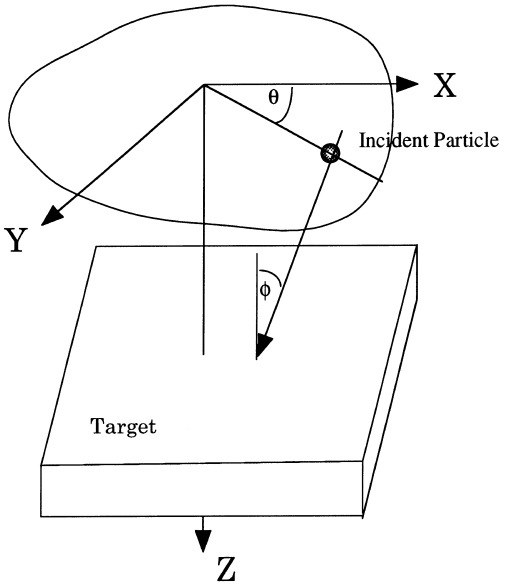

Fig. 3. Schematic view of sputtering simulation system.

Table 1
Target crystal and incident energy

Crystal size (nm) [a]	No. of atoms	Face	Incident energy (eV)
$2.020 \times 1.943 \times 2.759$	1440	(0 0 1)	50,100
$2.468 \times 2.575 \times 1.814$	1540	(0 1 0)	50
$3.590 \times 3.679 \times 1.814$	3200	(0 1 0)	100
$4.488 \times 4.664 \times 4.783$	12960	(0 0 1)	300

[a] The size of the initial structure is listed. The z-length is the thickness of the crystal plate.

These sizes were chosen so that the lattice defects created during the sputtering process were confined within a single simulation cell.

The crystal structure at the start was a structure obtained by 2 ps of NPT dynamics at 300 K. The incident Be atom was placed about 6 Å above the target crystal. Random fluctuations were given to x- and y-coordinates of the incident atom. Time duration of each simulation was 2 ps. The time increment Δt used in the integration of the equations of motions was initially chosen by the condition $v_0\ \Delta t \leqslant 0.03$ Å, where v_0 is the incident velocity, and it was set to be 0.5 fs eventually after thermalization. The interatomic forces were truncated at 6 Å.

Except for the 300 eV simulation, we ran 128 or 192 separate dynamics for each set of simulation conditions, the fewer 128 run applied only to normal incidence. The 300 eV simulation involves 64 runs. Therefore, the total number of the dynamics runs carried out for the present work amounts to 3648.

4. Results and discussion

Table 2 summarizes the statistics of our simulation. The results are compared with experimental estimates in Fig. 4 for the case of normal incidence. The agreement between our simulation and Bohdansky's estimate [11] is generally good, though better statistics is needed for fully quantitative comparison. Bohdansky's estimate itself shows some deviation from the actual experimental value of Guseva et al. at 1 keV [12]. (Real experimental yield is not available other than at 1 keV.)

Angle dependence of the sputtering yield is shown in Fig. 5, in which Monte Carlo simulation results by TRIM.SP [13] and 1 keV experimental results of Guseva et al. [12] are also plotted. It should be noted in this figure that the experimental sputtering yield includes the reflection coefficient while the computational yields do not contain the reflection part. Fairly good agreement is seen between the MD and TRIM.SP results. Direct comparison with the experimental results is not relevant due to the energy difference but general trend is similar between the simulation and experimental results. An interesting feature of the MD results in Fig. 5 is the noticeable difference between the yields of the (0 0 1) and (0 1 0) surfaces. The difference is statistically insignificant at small incident angles but it becomes distinct at larger angles, especially at 60°. The MD results indicate that the (0 1 0) surface is more susceptible to the sputtering than the (0 0 1) surface.

A noticeable difference between the MD and TRIM.SP results is observed in the reflection coefficient. As seen from Table 2 the reflection coefficient becomes unity at the incident angle of 75° in the 50 and 100 eV collision. The TRIM.SP prediction [13] is from 0.7 to 0.8

Table 2
Calculated sputtering yield (upper entry) and reflection coefficient (lower entry) [a]

Angle (deg)	(0 0 1) Face		(0 1 0) Face	
	50 eV	100 eV	50 eV	100 eV
0	0.016 (0.022)	0.094 (0.052)	0.086 (0.059)	0.102 (0.053)
	0 (0)	0 (0)	0 (0)	0 (0)
30	0.068 (0.036)	0.250 (0.069)	0.151 (0.052)	0.313 (0.075)
	0 (0)	0.005 (0.010)	0.016 (0.018)	0.021 (0.021)
45	0.339 (0.079)	0.703 (0.101)	0.448 (0.076)	0.823 (0.101)
	0.120 (0.047)	0.063 (0.035)	0.177 (0.055)	0.073 (0.038)
60	0.010 (0.015)	0.693 (0.118)	0.234 (0.063)	1.010 (0.136)
	0.938 (0.035)	0.484 (0.072)	0.771 (0.061)	0.432 (0.072)
75	0 (0)	0 (0)	0 (0)	0 (0)
	1.0 (0)	1.0 (0)	1.0 (0)	1.0 (0)

[a] The error estimate of 95.4% confidence level (i.e., $2\sigma/N^{1/2}$ with σ and N being the standard deviation and the number of dynamics runs, respectively) is shown in parentheses. (0 0 1)face, 300 eV, normal incidence: s.y. = 0.266 (0.127), r.c. = 0 (0).

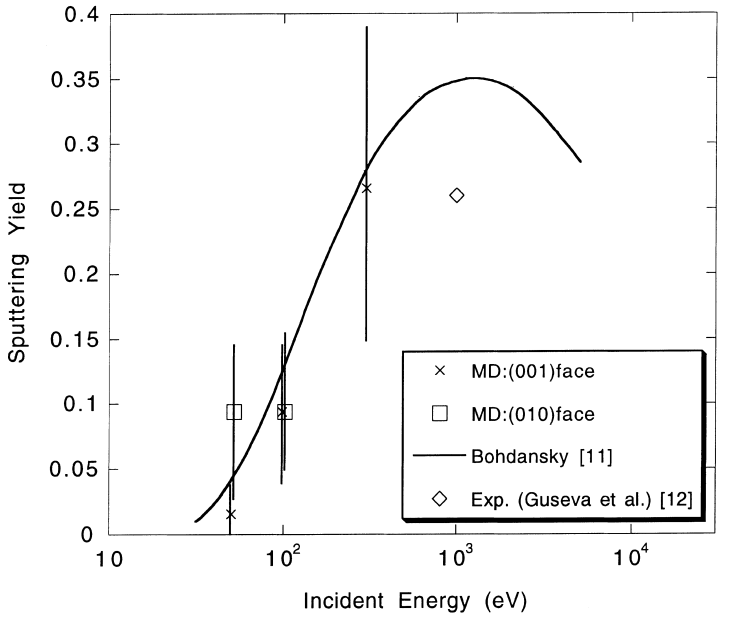

Fig. 4. Dependence of sputtering yield at normal incidence on incident energy. The error bar on the MD point corresponds to the 95.4% confidence level (Table 2).

in this angle and energy range. In general MD reflection coefficients at grazing angles are considerably enhanced as compared to the TRIM.SP prediction. Experimental check is difficult because the reflection and sputtering cannot be distinguished in the case of the self-sputtering. Nevertheless, the difference is interesting and worth further investigation.

We have made additional analyses on sputtered atoms in order to get more information about the sputtering process. Investigation of the initial position of

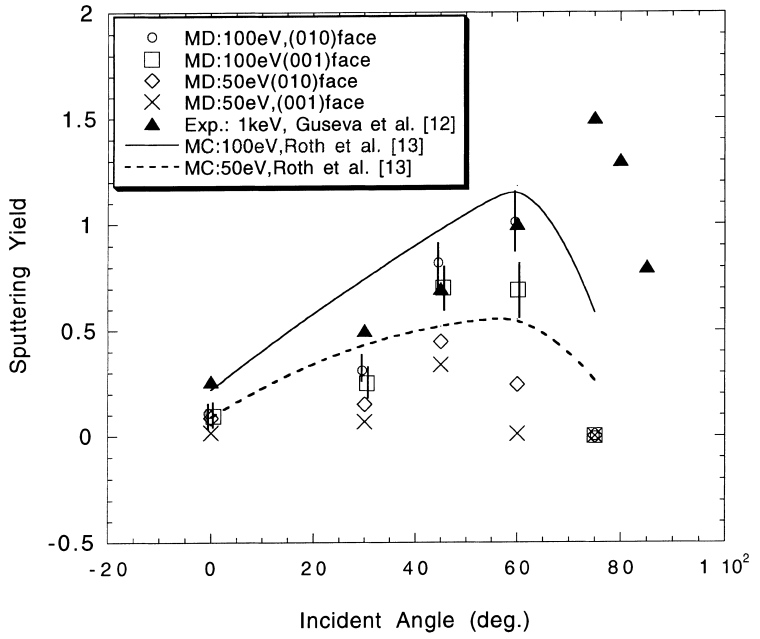

Fig. 5. Dependence of sputtering yield on incident angle. Error bars on the MD point are partly omitted for clarity. The MC curves correspond to $E_s = 2.0$ eV [13].

sputtered atoms has shown that all the sputtered atoms were initially located in the first layer of the crystal surface. The time at which each sputtered atom took off the surface can also be calculated. That time has turned out to be less than 100 fs. Only a few atoms had the takeoff time longer than 100 fs, with the longest time being ca. 120 fs.

5. Concluding remarks

We have presented an MD evaluation of Be self-sputtering in the present paper. The agreement between the simulation and experimental results indicates that fairly good evaluation is possible by the MD approach for the physical sputtering yield of plasma facing materials. An important factor to obtain good estimates is the interatomic potential, especially at its high energy region.

Small but distinct dependence of the sputtering yield on the crystal surface has been found, especially at larger incident angles. This effect causes a complication in the MD evaluation of sputtering. However, it is not a serious problem as the effect observed is weak. An interesting finding worth further investigation is the significantly enhanced MD reflection coefficients at grazing angles as compared to the TRIM.SP prediction.

Much more effort is obviously needed to establish the MD simulation as a practical tool of sputtering evaluation. In this direction we are now extending our work to He–BE and D–Be sputtering.

Acknowledgements

The authors would like to appreciate Dr. Y. Seki, Dr. Ohta, Director, Dr. Nagashima, Deputy Director, Department of Fusion Engineering Research, Japan Atomic Energy Research Institute for their great support in this work.

References

[1] R.E. Stoller, J. Nucl. Mater. 233–237 (1996) 999.
[2] J.P. Jacobs, M.A. San Miguel, L.J. Alvarez, P.B. Giral, J. Nucl. Mater. 232 (1996) 131.
[3] H.M. Urbassek, Nucl. Instr. and Meth. B 122 (1997) 427.
[4] P. Huxley, D.B. Knowles, J.N. Murrell, J.D. Watts, J. Chem. Soc. Faraday Trans. 280 (1984) 1349.
[5] E. Blaisten-Barojas, S.N. Khanna, Phys. Rev. Lett. 61 (1988) 1477.
[6] M. Igarashi, M. Khantha, V. Vitek, Philos. Mag. B 63 (1991) 603.
[7] D.E. Harrison, J. Appl. Phys. 52 (1981) 1499.
[8] W.J. Hehce, L. Radom, P. Schleyer, J.A. Pople, Ab Initio Molecular Orbital Theory, Wiley, New York, 1986.
[9] H.C. Andersen, J. Chem. Phys. 72 (1980) 2384.
[10] Written by S. Kuwajima mainly at CRC Research Institute, and distributed now by Nano Simulation Associates.
[11] J. Bohdansky, Nucl. Instr. and Meth. B 2 (1984) 587.
[12] M.I. Guseva, S.N. Korshunov, V.M. Gureev, Y.V. Martinenko, V. E. Neumoiin, V.G. Stoljarova, J. Nucl. Mater. 241–243 (1997) 1117.
[13] J. Roth, W. Eckstein, J. Bohdansky, J. Nucl. Mater. 165 (1989) 199.